# Supporting Information

## Calculation method

First-principles calculations are performed using the Vienna Ab initio Simulation Package (VASP) to investigate the NITRR process on the $SmCoO_3$(111) surface. [1-4] The valence-core electrons interactions are treated by Projector Augmented Wave (PAW) potentials and the electron exchange correlation interactions are described by the generalized gradient approximation (GGA) with the Perdew-Burke-Ernzerhof (PBE) functional.[5-6] Considered long-range interaction at the interface, Van der Waals interactions are considered using DFT-D3 correlation.[7] To avoid interaction from other slabs, a vacuum of 20 Å is added along z direction. The convergence criterion of geometry relaxation is set to 0.03 eV•Å$^{-1}$ in force on each atom. The energy cutoff for plane wave-basis is set to 500 eV. The K points are sampled with $3\times3\times1$ by Monkhorst-Pack method.[8]

Gibbs free energy change ($\Delta G$) is evaluated based on the computational hydrogen electrode (CHE) model, which takes one-half of the chemical potential of gaseous hydrogen under standard conditions as the free energy of the proton-electron pairs. $\Delta G$ is calculated by the following equation[9]:

$$\Delta G = \Delta E + \Delta E_{ZPE} - T\Delta S + neU$$

where $\Delta E$, $\Delta E_{ZPE}$, $\Delta S$ are the reaction energy from DFT calculation, the correction of zero-point energy and the change of simulated entropy, respectively. T is the temperature (T = 300 K). $n$ and U are the number of transferred electrons and applied potential respectively.

## Experimental Method

**Materials**： Disodium phosphate ($Na_2HPO_4$), sodium dihydrogen phosphate ($NaH_2PO_4$), Cobaltous nitrate hexahydrate ($Co(NO_3)_2 \cdot 6H_2O$), Samarium(III) nitrate hexahydrate ($Sm(NO_3)_3 \cdot 6H_2O$), cetyl trimethyl ammonium bromide (CTAB), Urea ($CO(NH_2)_2$), Ammonium fluoride ($NH_4F$)and polyvinylpyrrolidone (PVP) are

purchased from Aladdin Ltd (Shanghai, China). Sulfanilamide ($C_6H_8N_2O_2S$) is bought from Heowns technology Co., Ltd. N,N-Dimethylformamide (DMF), sodium nitrate ($NaNO_3$), sodium nitrite ($NaNO_2$), N- (1-naphthyl) ethyl diamine dihydrochloride ($C_{12}H_{14}N_2.2(HCl)$), phosphoric acid ($H_3PO_4$), ammonium chloride ($NH_4Cl$), sodium hypochlorite solution (NaClO), 4-dimethylaminobenzaldehyde ($C_9H_{11}NO$), sodium nitroferricyanide dihydrate ($C_5FeN_6Na_2$-O·$2H_2O$), hydrazine monohydrate ($N_2H_4$·$H_2O$), hydrogen peroxide ($H_2O_2$, 3 wt%), hydrochloric acid (HCl), sulfuric acid ($H_2SO_4$), sodium hydroxide (NaOH), salicylic acid ($C_7H_6O_3$), trisodium citrate dihydrate ($C_6H_5Na_3O_7$- $2H_2O$) and ethanol ($C_2H_5OH$) are purchased from Kelong chemical Ltd (Chengdu, China). Sodium salicylate ($C_7H_5NaO_3$) is purchased from Fuchen chemical reagents Co., Ltd (Tianjin, China). Nafion solution (5 wt%) is purchased from Sigma-Aldrich Chemical Reagent Co., Ltd. Deionized water is purified through a Millipore system.

**Synthesis of SmCoO$_3$ nanofibers:** 1.12 g of PVP (Mw=1,300,000 g mol$^{-1}$) is dissolved in 8 ml ethanol. 1.4332 g of $Sm(NO_3)_3$·$6H_2O$ and 0.9312g of $Co(NO_3)_2$·$6H_2O$ are dissolved in 10 mL DMF. The above two solutions are separately stirred for 45 minutes and then the above two solutions are mixed and stirred for 24 h. After that, the mixture is spun into nanofibers at a high voltage of 18 kV. After electrospinning, the fibers are collected and heat treated at 200 °C for 1 h and consecutively sintered at 700 °C for 1 h, which are then naturally cool to room temperature to get the SmCoO$_3$ nanofibers.

**Synthesis of Sm$_2$O$_3$ nanorod:** 0.89 g of Sm(NO$_3$)$_3$·6H$_2$O, 0.6g of Urea, 0.22 g of NH$_4$F and 2.78 g of CTAB are dissolved in 50 ml distilled water under magnetic stirring to obtain 0.04 M solution. Ammonia solution is added dropwise to maintain the pH value to 9–10. T Mixture is transferred into autoclave of 100 ml capacity sealed and maintained at 140 °C for 12 h natural cooling to room temperature. The obtained precipitate is separated by centrifugation, washed with distilled water and ethanol several times and calcined at 600 °C for 1 h.

**Synthesis of Co$_3$O$_4$ nanorod: 0.**582 g of Co(NO$_3$)$_2$·6H$_2$O, 0.6 g of Urea, 1 g of PVP (ditto) and 0.22 g of NH$_4$F are dissolved in 50 ml distilled water under magnetic stirring to obtain 0.04 M solution. Mixture is transferred into autoclave of 100 ml capacity sealed and maintained at 120 °C for 4 h natural cooling to room temperature. The obtained precipitate is separated by centrifugation, washed with distilled water and ethanol several times and calcined at 350 °C for 3 h.

**Material characterizations**： X-ray diffraction (XRD) analysis is performed by a Rigaku Smartlab with the radiation of Cu Kα. The sample morphology is photographed by ZEISS Gemini SEM 300 scanning electron microscope. The acceleration voltage is 3 kV during topography shooting and 15 kV during energy spectrum mapping shooting. The detector is SE2 secondary electronic detector. The transmission electron microscopy (TEM) and high-resolution TEM (HRTEM) images of sample are obtained using FEI F30 equipment with the accelerating voltage of 300 kV. X-ray photoelectron spectrometer (Thermo Fischer, ESCALAB Xi+) is used for XPS test. The excitation source is Al Ka ray (hv =1486.6 eV), and the working voltage

is 12.5 kV. The ion chromatography (IC) is tested by Thermo Scientific ICS-900. Nuclear magnetic resonance (NMR) is measured on a Bruker 400 MHz instrument.

**Working electrode preparation**: 5 mg of catalysts are grinded into powder and added into a mixed solution containing 635 μL ethanol, 325 μL deionized water and 40 μL of 5 wt% Nafion solution, followed by 30 min ultrasonic dispersion to form a homogeneous suspension. Then, 20 μL of such suspension is dropped on a 1´1 cm$^2$ carbon paper and dried in ambient temperature.

**Electrochemical measurements**: All electrochemical tests are performed in an H cell with a Nafion membrane in the middle. A three-electrode system is used in the experiments. The working electrode is carbon sheet coated with catalyst, and the counter electrode is platinum tablet. The electrolyte of the anode is the same as that of the cathode. The reference electrode is saturated with Ag/AgCl/KCl. The neutral electrolyte is 0.1 M PBS (prepared by $Na_2HPO_4$ and $NaH_2PO_4$) solution with pH=7. When the electrolyte is alkaline, the reference electrode is Hg/HgO/saturated KOH. The neutral electrolyte is 0.1 M PBS (prepared by $Na_2HPO_4$ and $NaH_2PO_4$) solution with pH=7, and the alkaline electrolyte is 0.1 M KOH solution with pH=13. $NaNO_3$ is added to the electrolyte after high temperature impurity removal as the N source.

In 0.1 M PBS with 0.1 M $NaNO_3$ electrolyte, the voltage of the relative reference electrode (Ag/AgCl) is converted into the voltage of the relatively reversible hydrogen electrode (RHE) by formula (1):

$$E(RHE) = 0.0591 \times PH + E(Ag/AgCl) + 0.197\,V \tag{1}$$

In 0.1 M KOH+0.1 M NaNO$_3$ electrolyte, the voltage of the relative reference electrode (Hg/HgO) is converted into the relatively reversible hydrogen electrode voltage (RHE) by formula (2):

$$E(RHE) = 0.0591 \times PH + E(Hg/HgO) + 0.865\,V \qquad (2)$$

Linear sweep voltammetry (LSV) is used to compare the same electrolyte with and without nitrate at 5 mV s$^{-1}$ scanning speed. Meanwhile, since nitrate concentration has a significant impact on NITRR process, LSV in the same electrolyte with different concentrations of nitrate is tested. Cyclic voltammetry (CV) tests are performed from 0.12 V to 0.22 V vs. Ag/AgCl at different scan rates of 20 mV s$^{-1}$, 40 mV s$^{-1}$, 60 mV s$^{-1}$, 80 mV s$^{-1}$ and 100 mV s$^{-1}$ without faradaic current. Solution resistance is determined by electrochemical impedance spectroscopy (EIS) at frequencies ranging from 0.1 to 10 kHz.

**Determination of ammonia (NH$_3$):** Ammonia produced in the NITRR process is colored by indophenol blue method and detected by the UV-vis spectroscopy. Due to the high concentration of the product, all electrolytes after electrolysis are diluted 10~40 times before color development. After 1 hour of electrolysis, 2 mL of electrolyte is taken from the cathode cell, followed by 2 mL colorant (containing salicylic acid, sodium citrate and sodium hydroxide), 1 mL of oxidant (0.05 M sodium hypochlorite), and 0.2 mL of catalyst solution (1 wt% sodium nitroferricyanide). Then, they are placed in the dark environment for 1 h, and the UV-vis spectra are measured in the wavelength range of 550 ~ 800 nm. The absorption intensity at 655 nm is substituted into the standard curve to quantify the ammonia yield.

**Determination of nitrite (NO$_2^-$):** The concentration of nitrite is measured by Griess reagent. 0.2 g of N- (1-naphthyl) ethyl-diamine dihydrochloride, 2.0 g of sulfa and 5.88 mL of phosphoric acid are dissolved in 100 mL of deionized water, and the Griess reagent is formed after being evenly stirred. After diluting the reacted electrolyte 10-20 times, 1 mL of the diluted electrolyte is taken by addition of 1 mL of Griess reagent and 2 mL of deionized water, and develop color stands in the dark environment of room temperature for 10 minutes. Magenta solution is obtained and UV-vis absorption spectra are tested in the ranges from 400 to 650 nm. The absorbance at 540 nm is substituted into the standard curve to obtain the concentration of nitrite.

**Determination of ammonia (NO$_3^-$):** The electrolytes are diluted to the detection range. In brief, 0.1 mL 1 M HCl and 0.01 mL 0.8 wt% sulfamic acid solution are added into 5 mL diluted electrolyte. The absorption spectrum is measured using a UV-Vis spectrophotometer and the absorption intensities at a wavelength of 220 nm and 275 nm are recorded. The final absorbance value is calculated by this equation: A = A220 nm – 2A275 nm. The calibration curve can be obtained through different concentrations of NaNO$_3$ solutions and the corresponding absorbance.

**Determination of hydrogen (H$_2$):** In the NITRR process, HER is a competitive reaction in cathode. H$_2$ is the product of HER process and can be detected by blowing the product after electrolysis in the cathode chamber into a gas chromatograph (GC). In order to reduce the experimental error caused by the different thermal conductivity of the gas, the carrier gas of the chromatography is nitrogen. Nitrogen is passed into the cathode electrolyte at a flowing rate of 30 mL min$^{-1}$, and GC collected the gas produced

by the reaction in the cathode chamber every 5 minutes. The hydrogen concentration can be obtained by integrating the characteristic peaks of hydrogen collected in the TCD detector.

**Calculations of faradaic efficiency (FE) and yield rate**: The yields of $NH_3$ and $NO_2^-$ are calculated by equation (3):

$$Yield = C \times V \div (t \times m_{cat.}) \tag{3}$$

The FE of $NH_3$ is calculated by equation (4):

$$FE_1 = 8 \times F \times C(NH_3) \times V \div (17 \times Q) \tag{4}$$

The FE of $NO_2^-$ is calculated by equation (5):

$$FE_2 = 2 \times F \times C(NO_2^-) \times V \div (46 \times Q) \tag{5}$$

The concentration of $H_2$ is measured by GC and TCD. The volume mole number n can be calculated according to formula (6):

$$n = P \times V' \div (R \times T) \tag{6}$$

The corresponding FE of $H_2$ can be calculated by equation (7):

$$FE_3 = n \times [H_2] \times F \times 2 \div Q \tag{7}$$

where C is the measured $NH_3$/$NO_2^-$ concentration, V the volume of electrolyte in the cathode chamber, t the time for which the potential is applied, $m_{cat.}$ the mass of catalyst loaded on the working electrode, F the Faraday constant (F=96485 C mol$^{-1}$), Q the charge applied, P the standard atmospheric pressure, V' the volume of gas through GC, R the universal gas constant, T the reaction temperature.

**$^{15}$N isotope labeling experiments**: Na$^{15}$NO$_3$ is used as N source for nitrate reduction isotope labeling experiment to verify the origin of as-synthesized ammonia. The purity of Na$^{15}$NO$_3$ is more than 98.5% and they are stored in a vacuum drying oven before being used. 0.1 M Na$^{15}$NO$_3$+0.1 M PBS as the electrolyte, the catalyst is subjected to $^{15}$NITRR for 20 h at the optimum voltage. To prepare the NMR sample, the pH of the electrolyte is adjusted to about 1 with 1 M H$_2$SO$_4$, then 0.5 mL electrolyte is added with 0.01 vol% DMSO and 0.1 mL D$_2$O, respectively. The $^1$H NMR spectrum of $^{15}$NH$_4^+$ (400 MHz) is determined. As a control, $^1$H NMR spectrum is tested after reaction in 0.1 M Na$^{14}$NO$_3$+0.1 M PBS electrolyte.
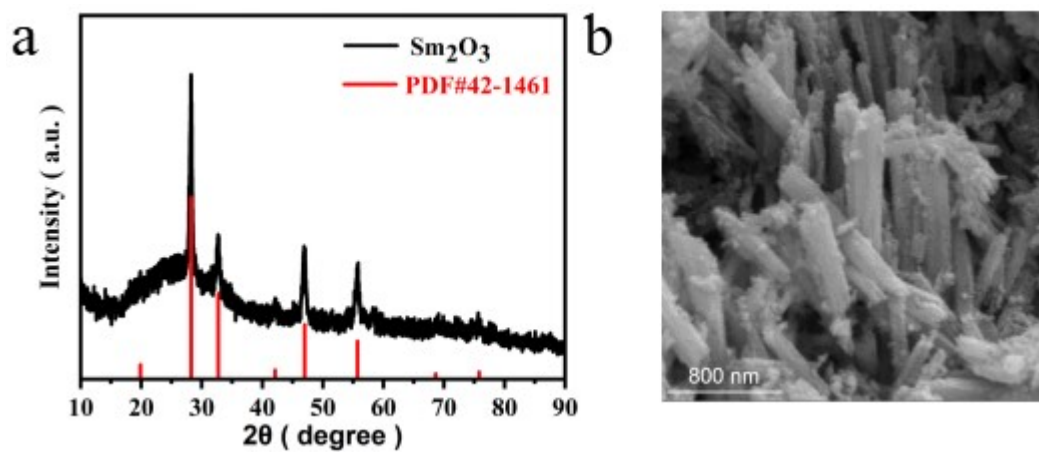
Fig. S1. (a) XRD pattern and (b) SEM image of $Sm_2O_3$
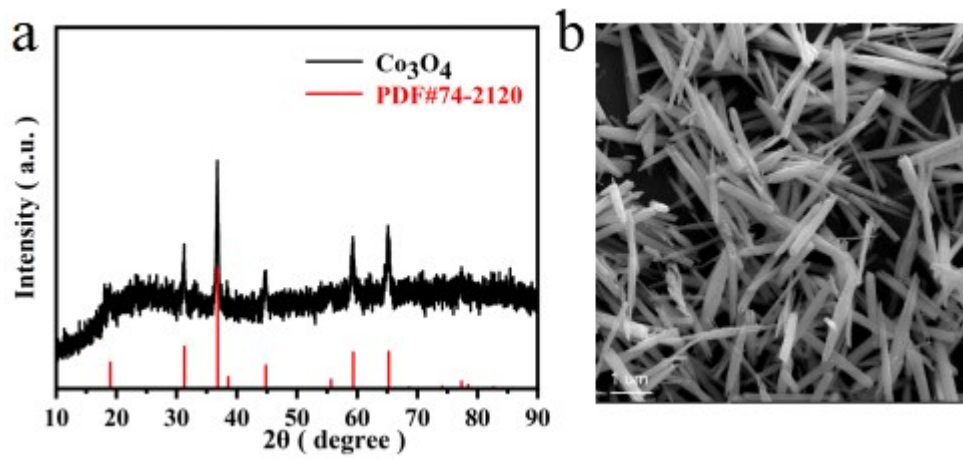
Fig. S2. (a) XRD pattern and (b) SEM image of $Co_3O_4$
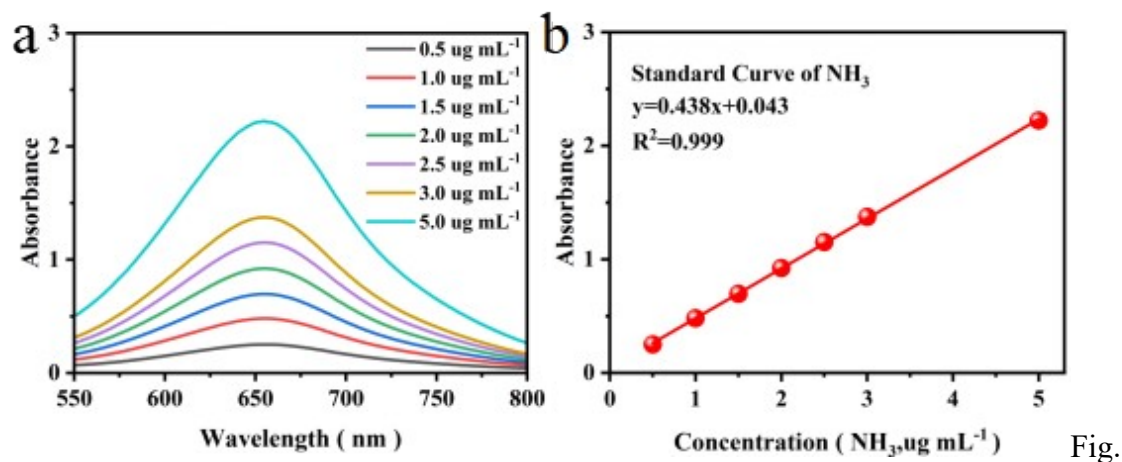
Fig. S3. (4) UV-vis absorption spectra of different concentrations of $NH_3$ stained with indophenol blue and (b) the corresponding calibration curve in 0.1 M PBS.
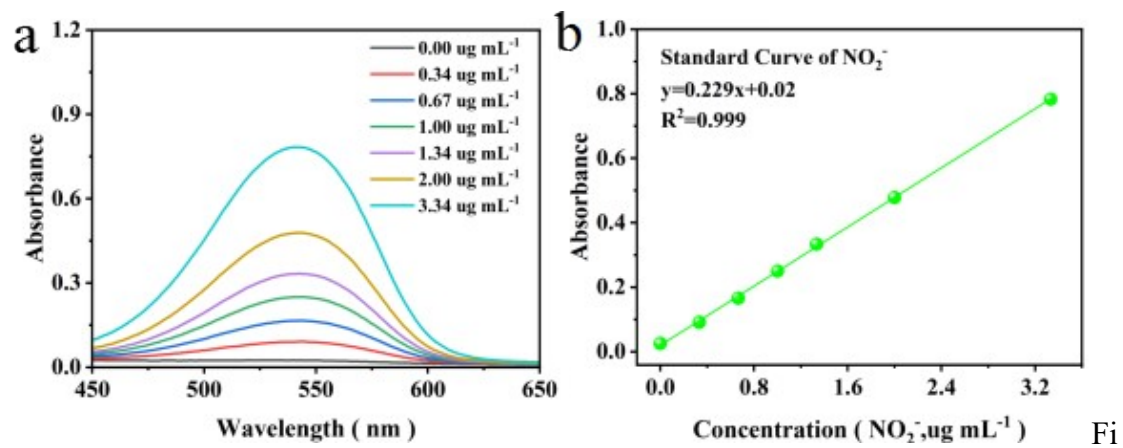
g. S4. (a) UV-vis absorption spectra of various concentrations of $NO_2^-$ after sitting for 20 minutes and (b) the corresponding calibration curve in 0.1 M PBS.
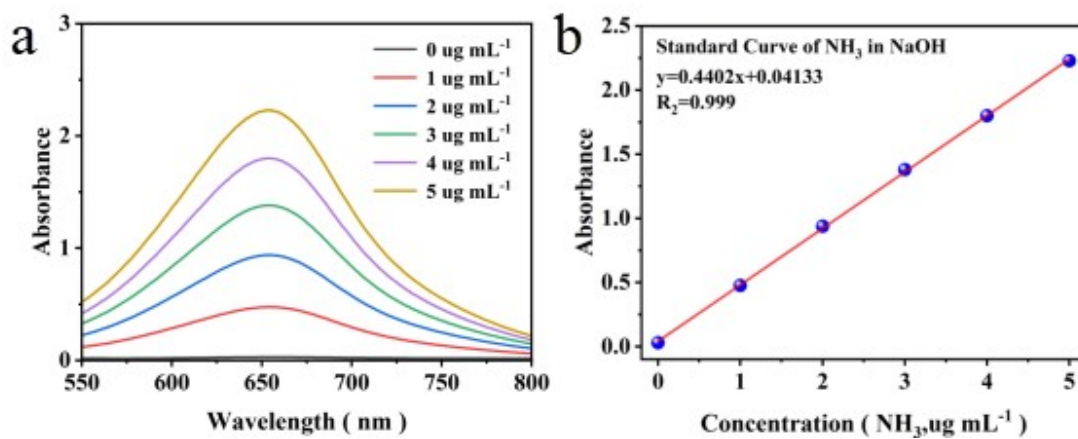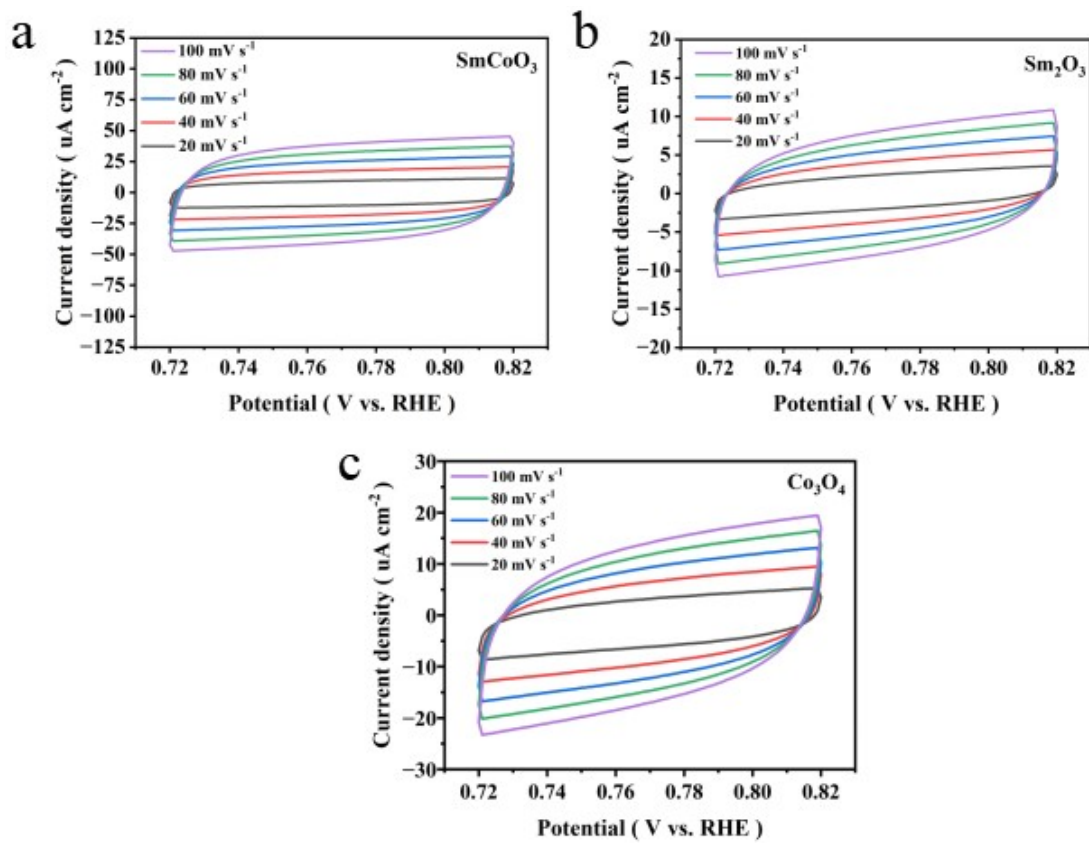
Fig. S5. (a) UV-vis absorption spectra of various concentrations of $NH_3$ after sitting

for 20 minutes and (b) the corresponding calibration curve in 0.1 M NaOH.
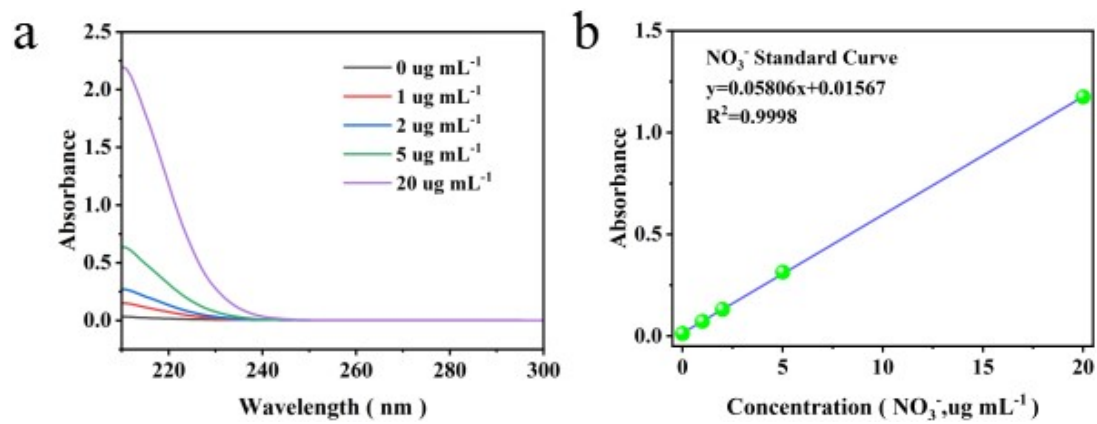
Fig. S6. (a) UV-vis absorption spectra of various concentrations of NO₃⁻ after sitting

for 20 minutes and (b) the corresponding calibration curve in 0.1 M PBS.

Fig. S7. (a-c) CV curves of different scan rates of SCO, Sm$_2$O$_3$ and Co$_3$O$_4$.
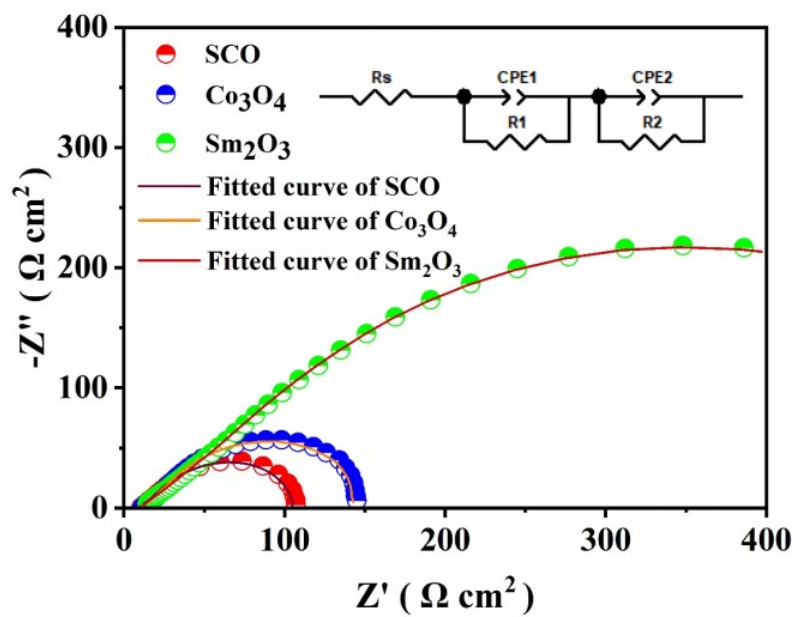
Fig. S8. Electrochemical impedance spectra and equivalent circuit of SCO, $Co_3O_4$ and $Sm_2O_3$
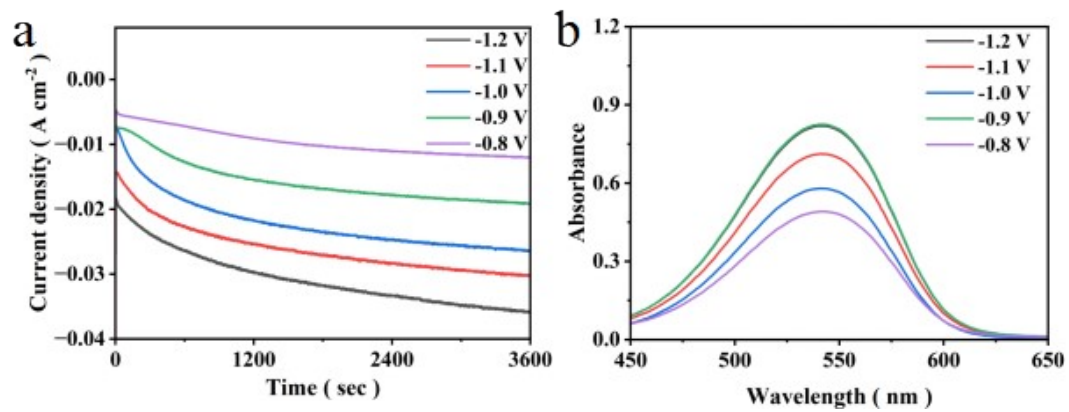
Fig. S9. (a) i-t curves for 1 h and (b) UV-vis absorption spectra of $NO_2^-$ (-0.8 and -0.9

V are diluted 10 times while others are diluted 20 times).
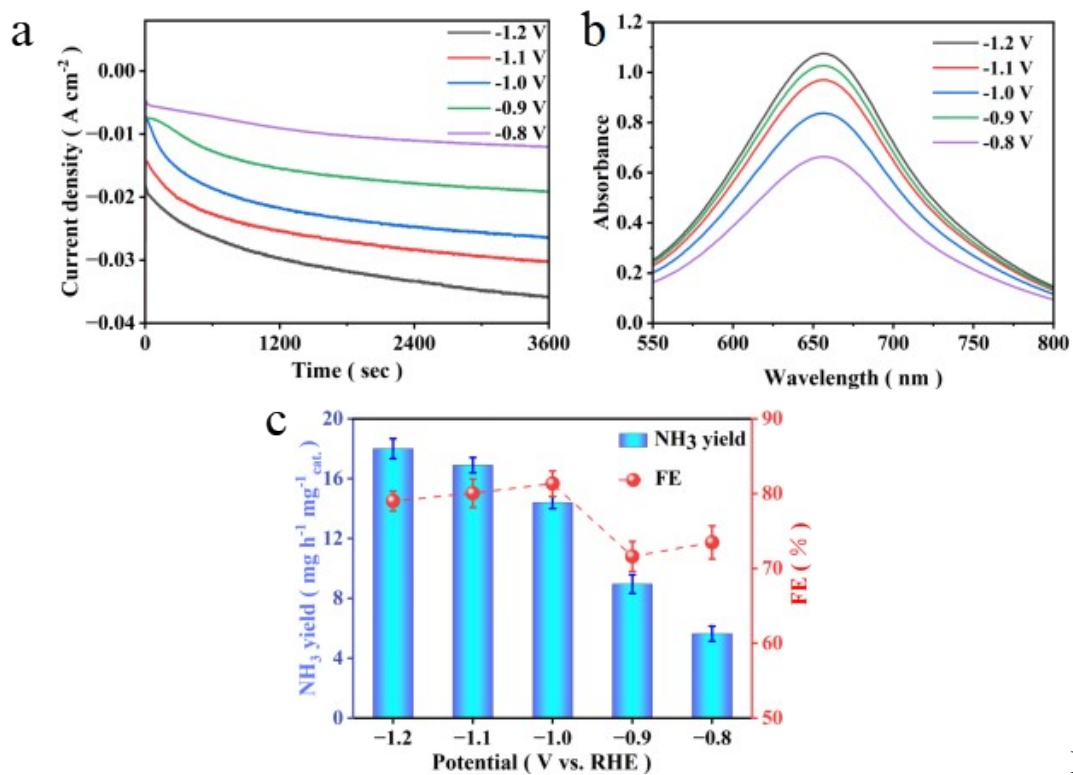
Fig. S10. (a) i-t curves for 1 h, (b) UV-vis absorption spectra of $NH_3$ (-0.8 and -0.9 V are diluted 10 times while others are diluted 20 times) and (c) $NH_3$ yield and FE of SCO.
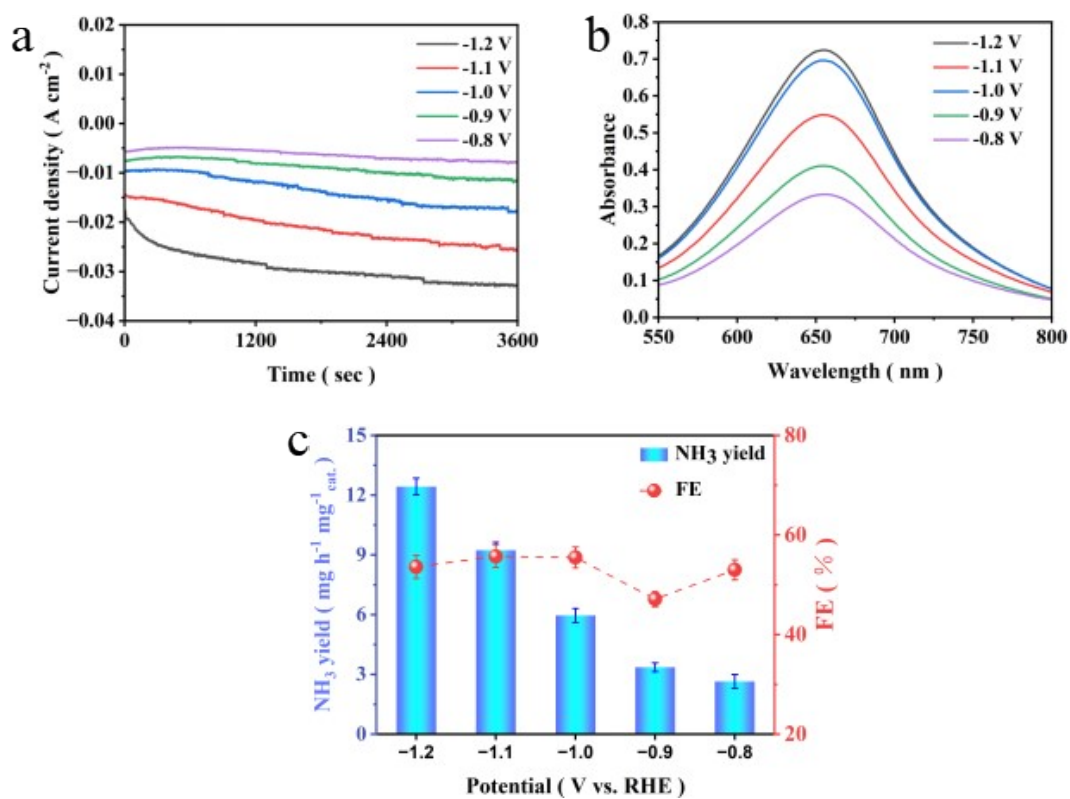
Fig. S11. (a) i-t curves for 1 h. (b) UV-vis absorption spectra of $NH_3$ (-0.8, -0.9 and -1.0 V are diluted 10 times while others are diluted 20 times) and (c) $NH_3$ yield and FE of $Sm_2O_3$.
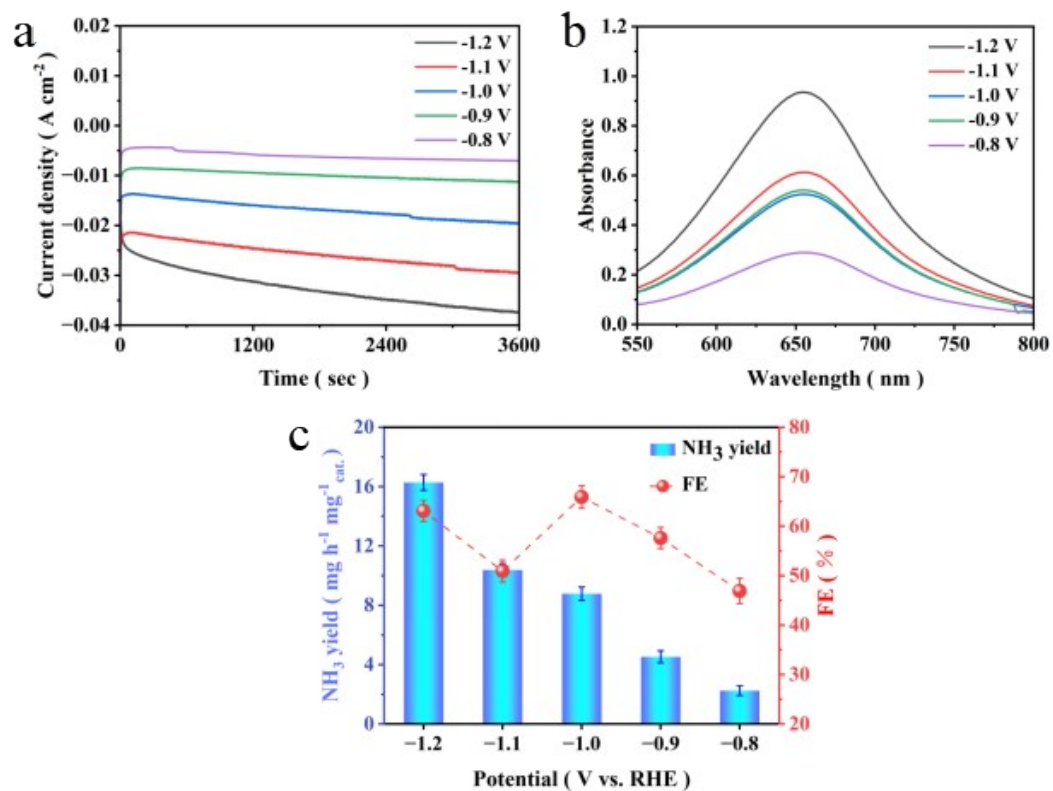
Fig. S12. (a) i-t curves for 1 h. (b) UV-vis absorption spectra of $NH_3$ (-0.8 and -0.9 V are diluted 10 times while others are diluted 20 times) and (c) $NH_3$ yield and FE of $Co_3O_4$.
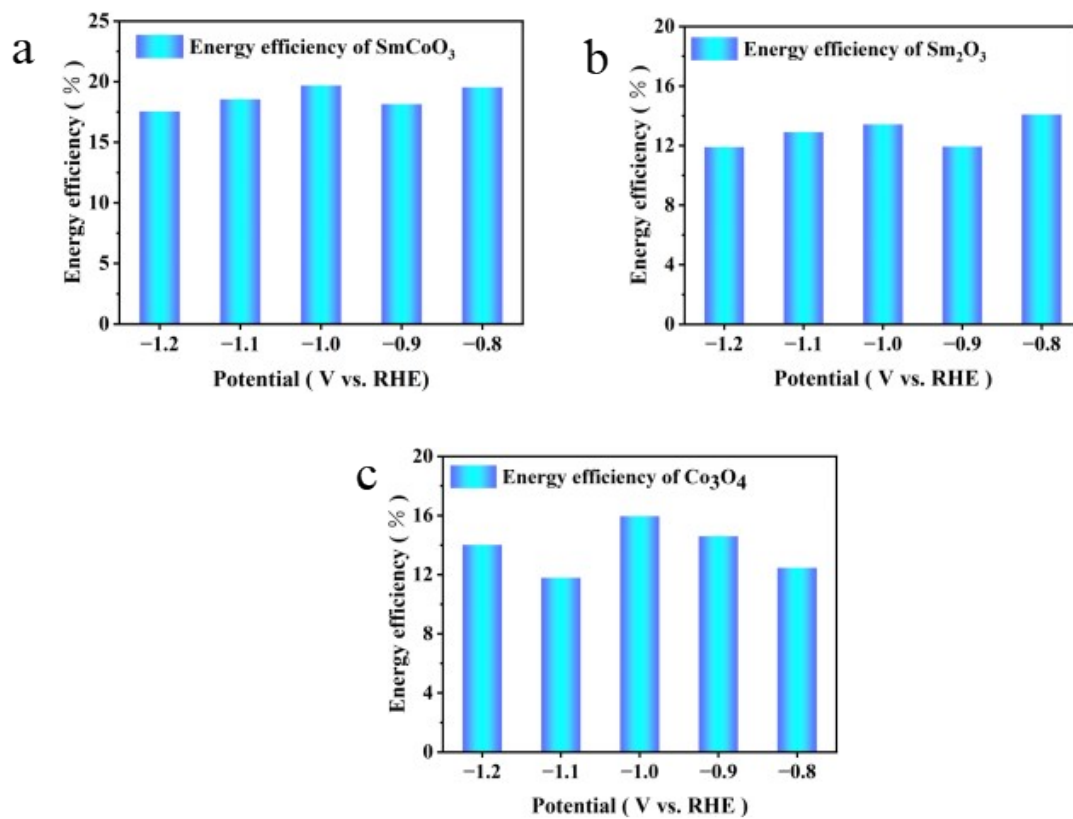
Fi

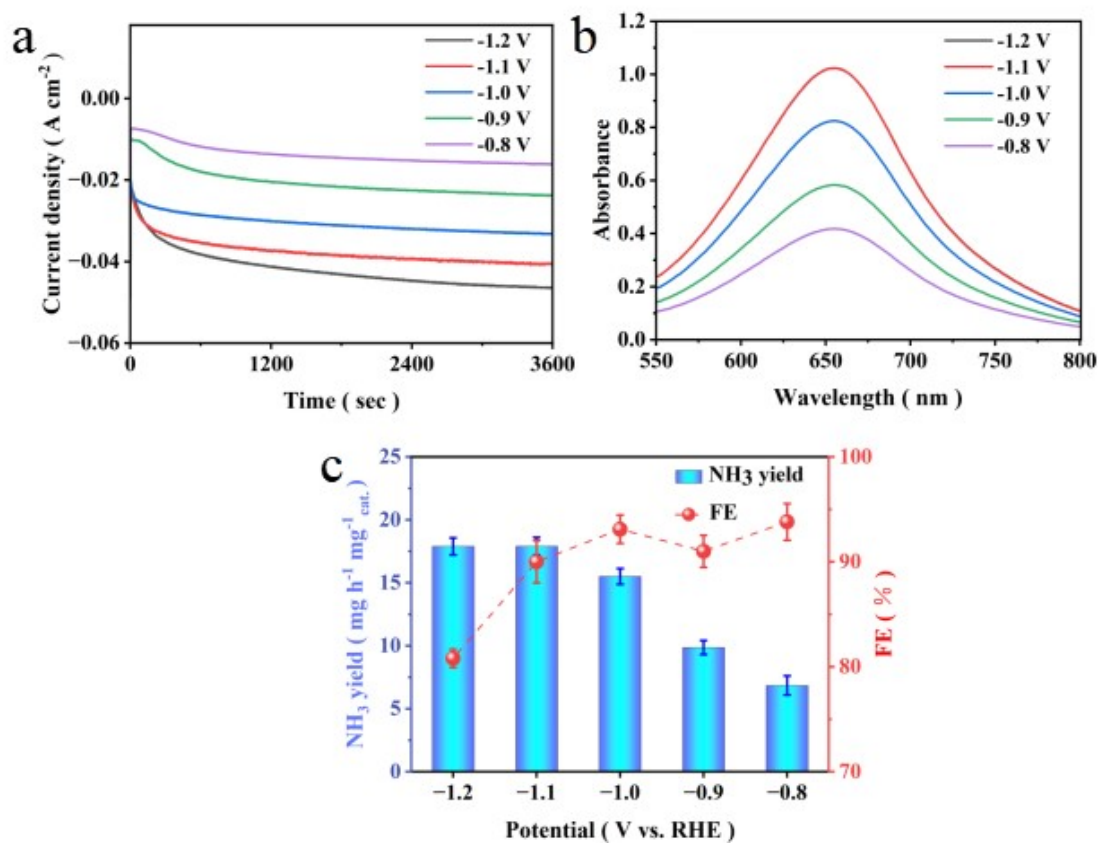g. S13. Energy efficiency of (a) SCO, (b) $Sm_2O_3$ and (c) $Co_3O_4$.

Fig S14. (a) i-t curves for 1 h. (b) UV-vis absorption spectra of $NH_3$ (all are diluted 20 times) and (c) $NH_3$ yield and FE of SCO in 0.1 M PBS+0.1 M $NO_2^-$.
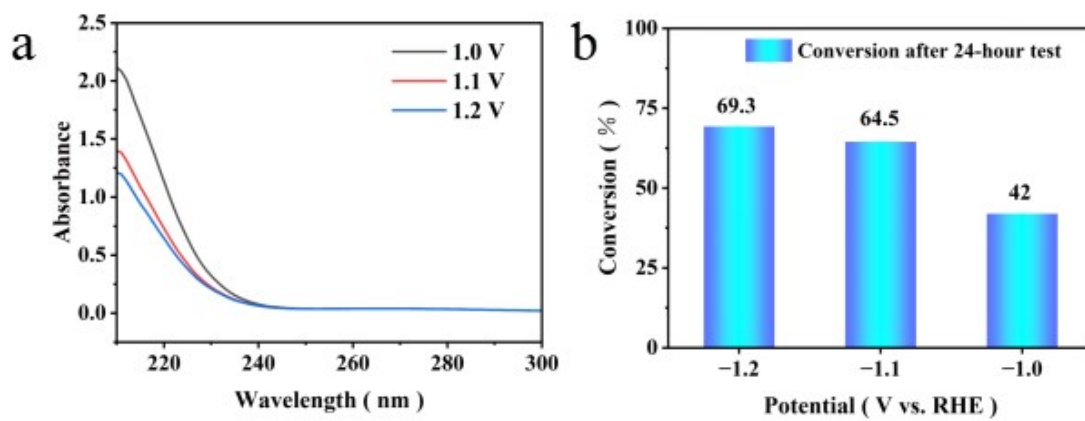
Fig. S15 (a) UV-vis absorption spectra of $NO_3^-$ after 24-hour test and (b) conversion of
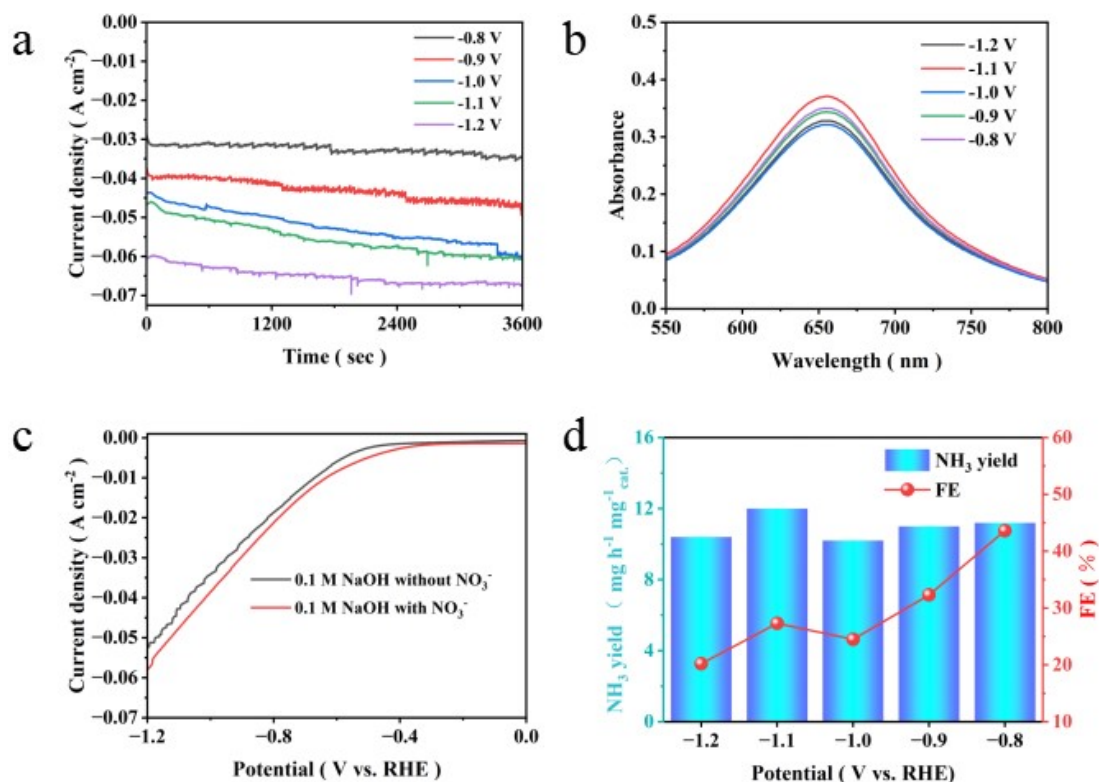
$NO_3^-$ after 24-hour test.

Fig. S16 (a) i-t curves for 1 h. (b) UV-vis absorption spectra of $NH_3$. (c) LSV curves of SCO tested in 0.1 M NaOH with and without 0.1 M $NO_3^-$ and (d) $NH_3$ yield and FE of SCO in 0.1 M NaOH+0.1 M $NO_3^-$.
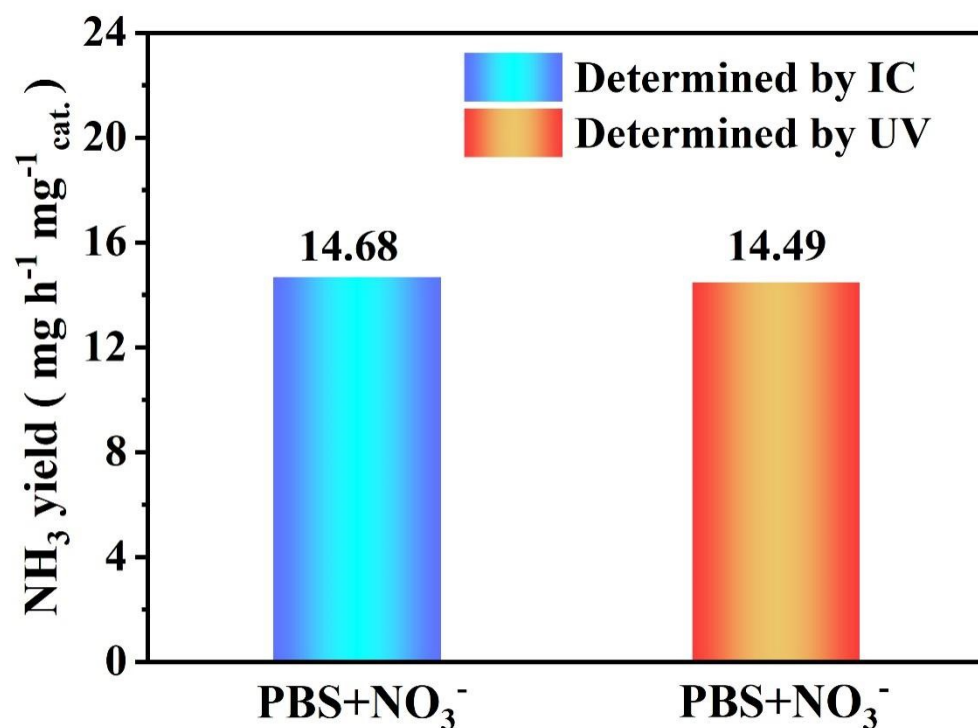
Fig. S17. The $NH_3$ yield rate detected using the IC method and UV method after 1-h electrolysis in 0.1 M PBS with 0.1 M $NO_3^-$ at -1.0 V over SCO.
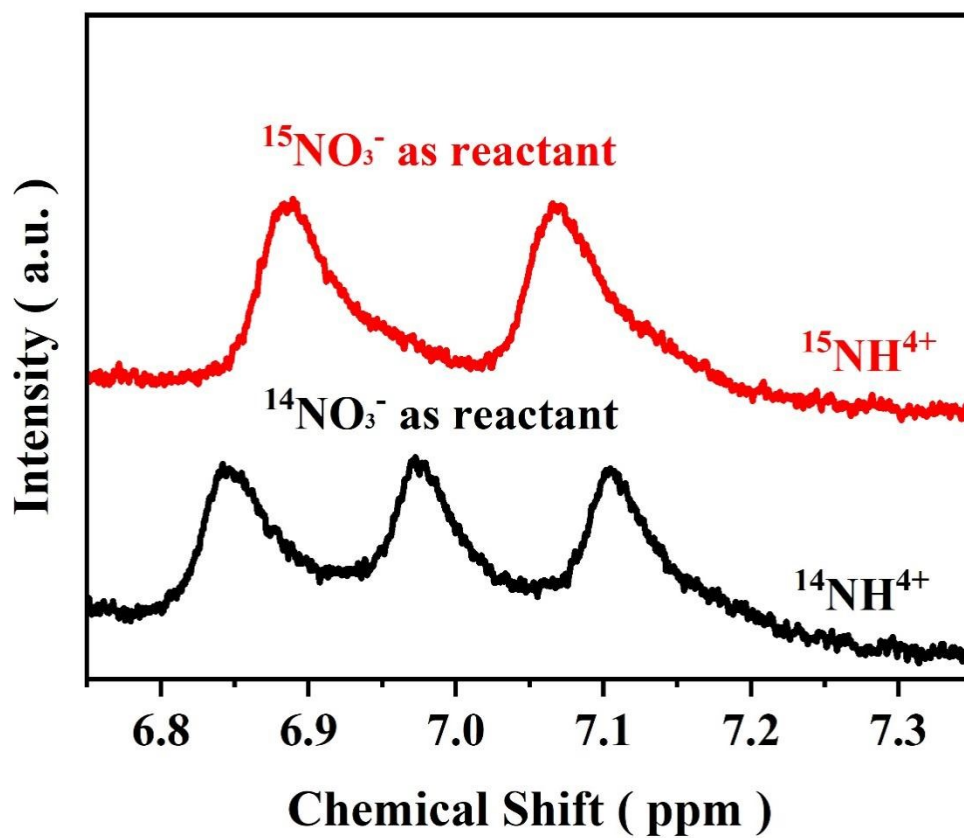
Fig. S18. $^1$H NMR spectra of electrolyte after NITRR using $^{15}NO_3^-$ and $^{14}NO_3^-$ as nitrogen sources, respectively.
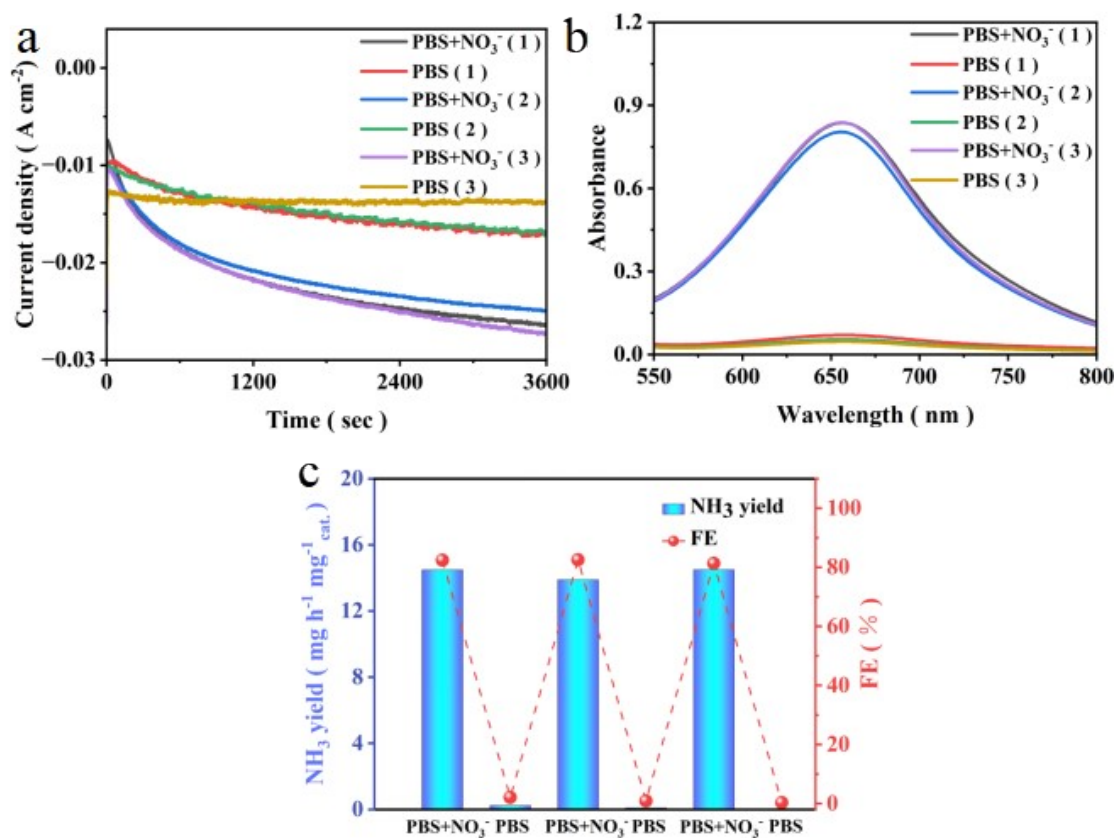
Fig. S19 (a) i-t curves for 1 h. (b) UV-vis absorption spectra of $NH_3$ and (c) $NH_3$ yields and FEs with alternating 1 h cycles in the PBS electrolyte with and without $NO_3^-$ for SCO.
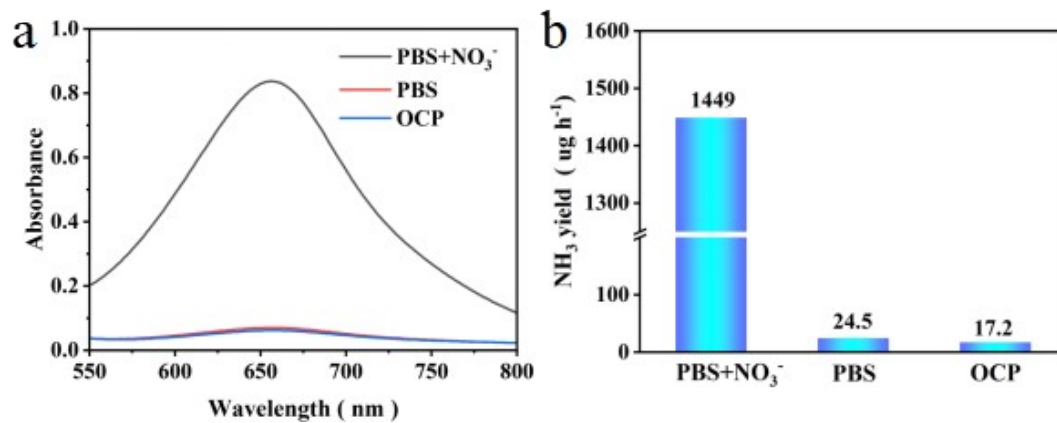
Fig. S20 (a) UV-vis absorption spectra of indophenol assays and (b) corresponding ammonia yield after 1-h electrolysis under different condition for SCO.
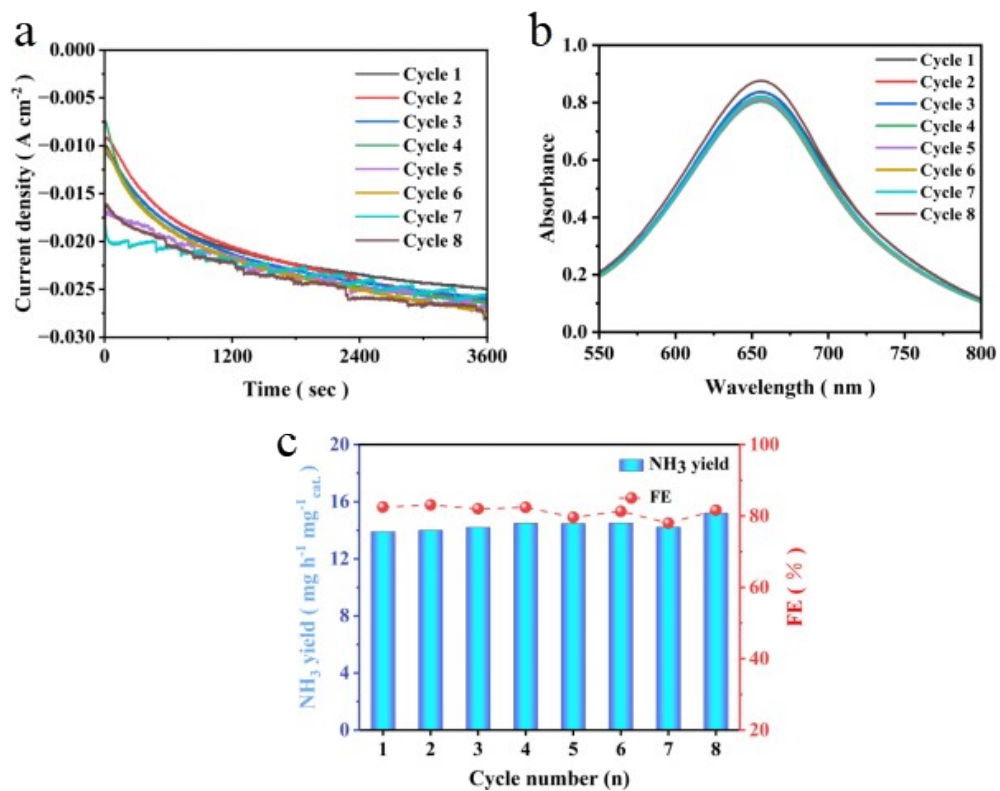
Fig. S21 (a) i-t curves for 1 h. (b) UV-vis absorption spectra of $NH_3$ of each cycle and (c) $NH_3$ yield and FE for 8 consecutive cycles of SCO in 0.1 M PBS with 0.1 M $NO_3^-$ electrolyte.
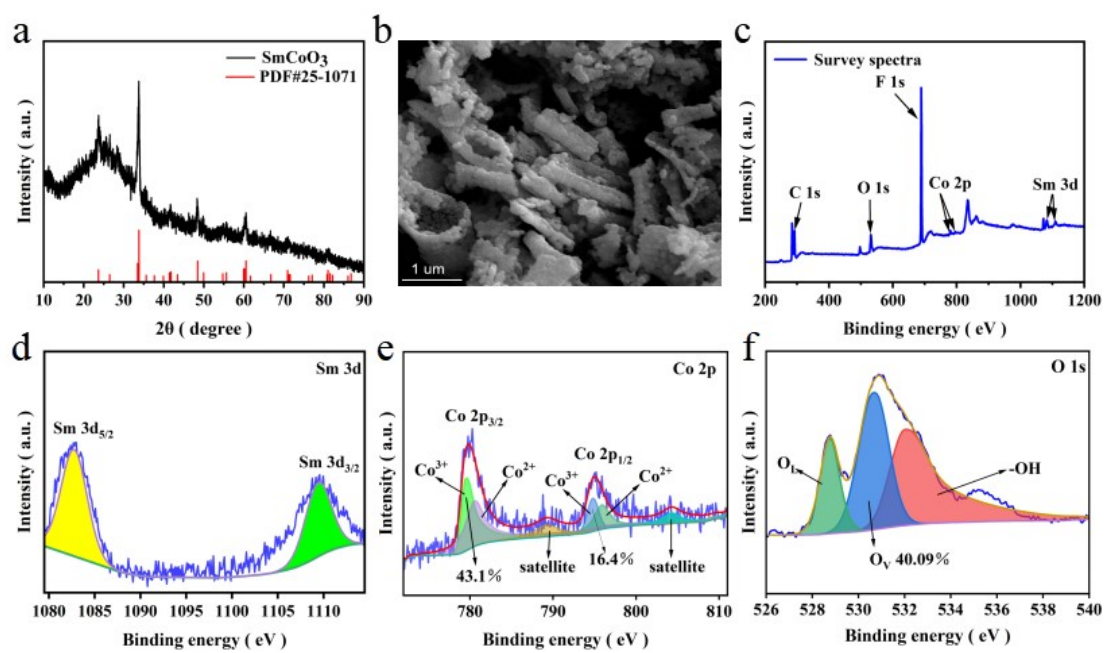
Fig. S22 (a) XRD pattern, (b) SEM image, (c) XPS survey spectrum and XPS spectra of (d)Sm 3d, (e) Co 2p and (f) O 1s of SCO after 24-h electrolysis.

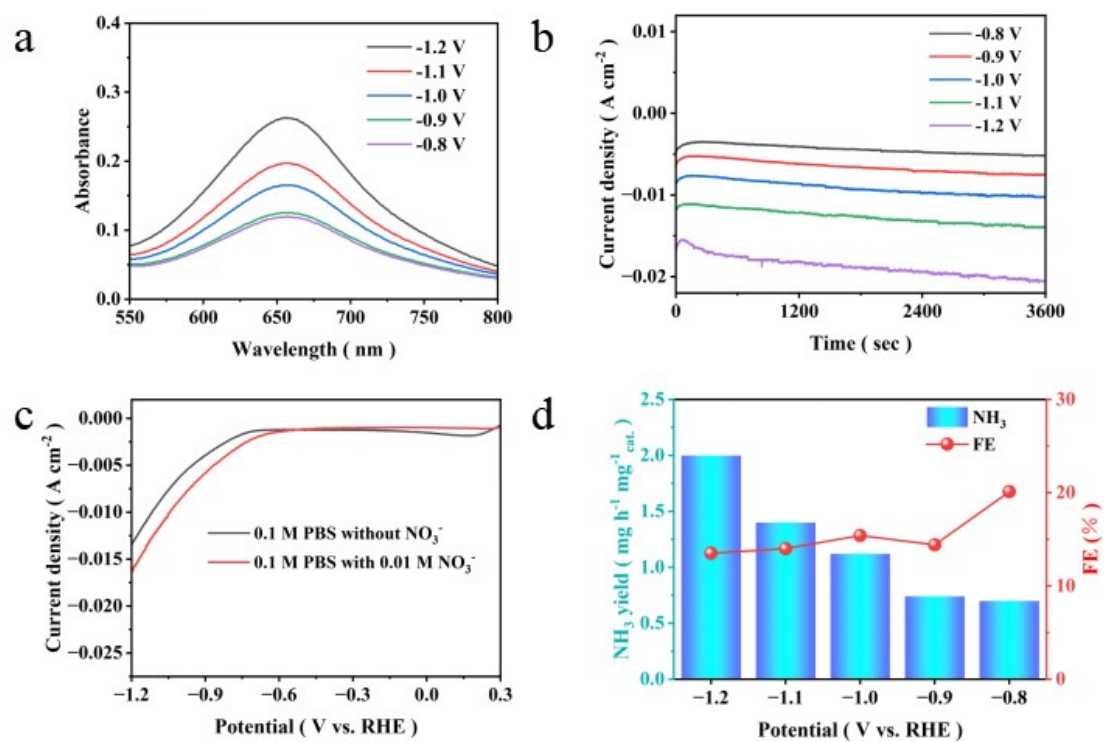Fig. S23 (a) i-t curves for 1 h. (b) UV-vis absorption spectra of NH$_3$. (c) LSV curves of SCO tested in 0.1 M PBS with and without 0.01 M NO$_3^-$ and (d) NH$_3$ yield and FE of SCO in 0.1 M PBS+0.01 M NO$_3^-$.
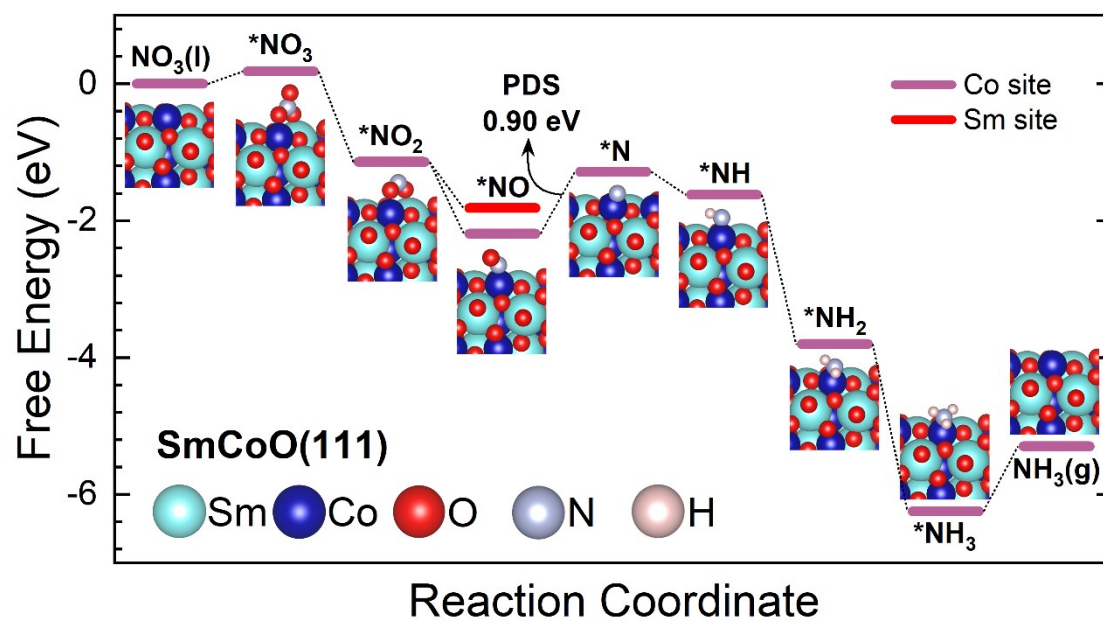
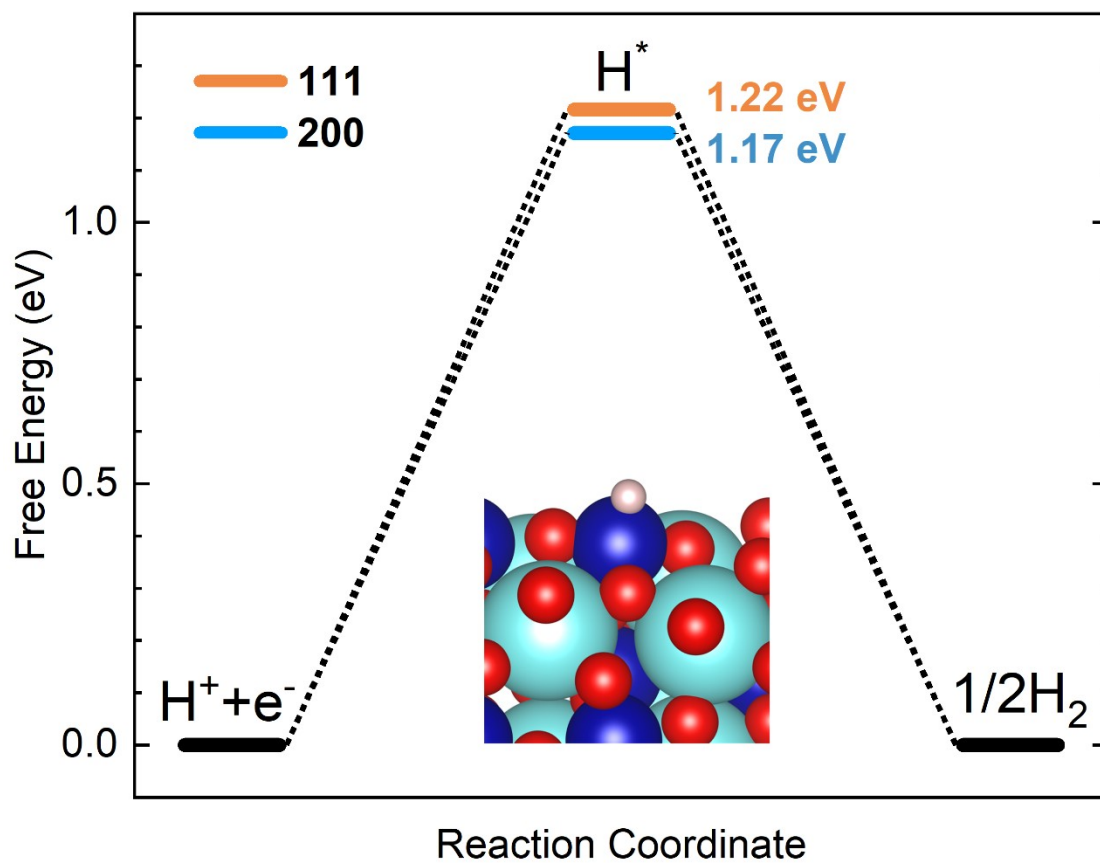**Fig. S24**. Calculated free energy profile of NO₃RR on the SmCoO₃(111) surface.

**Fig. S25**. Calculated free energy diagram for HER process on the SmCoO$_3$ (111) and (200) surfaces.

| Catalyst | Electrolyte | NH$_3$ yield (mg h$^{-1}$ mg$^{-1}_{cat.}$) | FE | Ref. |
|---|---|---|---|---|
| **SmCoO$_3$** | **0.1 M PBS +0.1 M NaNO$_3$** | **14.343 $\pm$ 0.404** | **81.31 $\pm$ 1.7** | **This work** |
| LaCrO$_3$ | 1 M Na$_2$SO$_4$ +0.5 M KNO$_3$ | 7.48 | 21.7 | 10 |
| LaMnO$_3$ | 1 M Na$_2$SO$_4$ +0.5M KNO3 | 14.96 | 49.1 | 10 |
| Co$_3$O$_4$@NiO HNTs | 0.5 M Na$_2$SO$_4$ + 200 ppm NO$_3^-$N | 0.118 | 54.97 | 11 |
| Pd nanodots on Zr-MOF | 0.1 M Na$_2$SO$_4$ + 500 ppm NaNO$_3$ | 0.287 | 58.1 | 12 |
| Cu (111) nanodisks | 0.1 M KOH + 0.01 M KNO$_3$ | 2.16 | 81.11 | 13 |
| Cu@ZrO$_2$ | 0.1 M PBS +0.1 M NaNO$_3$ | 15.4 | 67.6 | 14 |
| In-S-G | 0.1 M KOH + 0.1 M KNO$_3$ | 3.74 | 75 | 15 |
| RuNi-MOF | 0.1 M KOH + 0.1 M KNO$_3$ | 0.274 | 73 | 16 |
| Pd facets | 0.1 M NaOH+ 0.02 M NaNO$_3$ | 0.307 | 35 | 17 |
| NbO$_x$ | 0.5 M K$_2$SO$_4$ + 1000 ppm KNO$_3$ | 0.012 | 94.5 | 18 |
| Cu–Pd/C nanobelts | 0.1 M KOH + 0.01 M KNO3 | 0.221 | 62.3 | 19 |
| TiO$_{2-x}$ | 0.5 M Na$_2$SO$_4$ + 50 ppm NO$_3^-$N | 0.765 | 85 | 20 |

# References

1.  G. Kresse and J. Furthmüller, *Phys. Rev. B*, 1996, **54**, 11169.

2.  G. Kresse and J. Furthmüller, *Comput. Mater. Sci.,* 1996, **6**, 15-50.

3.  G. Kresse and J. Hafner, *Phys. Rev. B*, 1994, **49**, 14251-14269.

4.  M. Segall, P. J. Lindan, M. a. Probert, C. J. Pickard, P. J. Hasnip, S. Clark, M. Payne, *J. Phys.-Condes. Matter*, 2002, **14**, 2717.

5.  P. E. Blochl, *Phys. Rev. B*, 1994, **50**, 17953-17979.

6.  J. P. Perdew, J. A. Chevary, S. H. Vosko, K. A. Jackson, M. R. Pederson, D. J. Singh and C. Fiolhais, *Phys. Rev. B*, 1992, **46**, 6671-6687.

7.  S. Grimme, J. Antony, S. Ehrlich and H. Krieg, *J. Chem. Phys.*, 2010, **132**, 154104.

8.  H. J. Monkhorst and J. D. Pack, *Phys. Rev. B*, 1976, **13**, 5188-5192.

9.  J. Nørskov, J. Rossmeisl, A. Logadottir, L. Lindqvist, J. Kitchin, T. Bligaard and H. Jonsson, *J. Phys. Chem. B,* 2004, **108**, 17886-17892.

10. H. Zheng, Y. Zhang, Y. Wang, Z. Wu, F. Lai, G. Chao, N. Zhang, L. Zhang and T. Liu, *Small*, 2022, DOI: 10.1002/smll.202205625, e2205625.

11. Y. Wang, C. Liu, B. Zhang and Y. Yu, *Sci. China Mater.*, 2020, **63**, 2530-2538.

12. M. Jiang, J. Su, X. Song, P. Zhang, M. Zhu, L. Qin, Z. Tie, J. Zuo and Z. Jin, *Nano Lett.,* 2022, **22**, 2529-2537.

13. K. Wu, C. Sun, Z. Wang, Q. Song, X. Bai, X. Yu, Q. Li, Z. Wang, H. Zhang, J. Zhang, X. Tong, Y. Liang, A. Khosla and Z. Zhao, *ACS Mater. Lett.*, 2022, **4**, 650.

14. J. Xia, H. Du, S. Dong, Y. Luo, Q. Liu, J. S. Chen, H. Guo and T. Li, *Chem. Commun.*, 2022, **58**, 13811-13814.

15. F. Lei, W. Xu, J. Yu, K. Li, J. Xie, P. Hao, G. Cui and B. Tang, *Chem. Eng. J.*, 2021, **426**.131317

16. J. Qin, K. Wu, L. Chen, X. Wang, Q. Zhao, B. Liu and Z. Ye, *J. Mater. Chem. A*, 2022, **10**, 3963-3969.

17. J. Lim, C. Liu, J. Park, Y. Liu, T. Senftle and S. Lee, M. Hatzell, *ACS Catal.*, 2021, **11**, 7568-7577.

18. X. Wan, W. Guo, X. Dong, H. Wu, X. Sun, M. Chu, S. Han, J. Zhai, W. Xia, S. Jia, M. He and B. Han, *Green Chem.*, 2022, **24**, 1090-1095.

19. Z. Wang, C. Sun, X. Bai, Z. Wang, X. Yu, X. Tong, Z. Wang, H. Zhang, H. Pang, L. Zhou, W. Wu, Y. Liang, A. Khosla and Z. Zhao, *ACS Appl. Mater. Interfaces*, 2022, **14**, 30969-30978.

20. R. Jia, Y. Wang, C. Wang, Y. Ling, Y. Yu and B. Zhang, *ACS Catal.*, 2020, **10**, 3533-3540.